

Full Paper Proceedings of ISAG2019 ISBN: 978-975-461-564-7

www.isag-2019.yildiz.edu.tr

YILDIZ TECHNICAL UNIVERSITY 1911

INTERNATIONAL SYMPOSIUM ON
APPLIED GEOINFORMATICS
7-9 Nov. 2019 · Istanbul/Turkey

100 UNIVERSITY OF LATVIA ANNO 1919

YILDIZ TECHNICAL UNIVERSITY DAVUTPASA CONVENTION CENTRE
34220 ESENLER, ISTANBUL/TURKEY

+90 212 383 5287

isag-2019@yildiz.edu.tr



ISAG2019 – International Symposium on Applied Geoinformatics

All rights are reserved, especially the right to translate into foreign language or other processes - or convert to a machine language, especially for data processing equipment -without written permission of the publisher. The rights of reproduction by lecture, radio and television transmission, magnetic sound recording or similar means are also reserved.

Printed in Turkey-ISBN: 978-975-461-564-7

EDITOR
Prof. Dr. Bulent Bayram

10312- MAPPING SOIL SALINITY BY USING LANDSAT-8 OLI IMAGERY AND REGRESSION ANALYSIS OVER BONAB COUNTY OF EAST AZERBAIJAN PROVINCE IN IRAN, 504
***T.* Gorji, A. Yildirim, N. Hamzehpour, E. Sertel, A. Tanik**

10364- INVESTIGATION OF OPEN SOURCE GEO-INFORMATION INTEGRATION IMPACT ON OBJECT-BASED CLASSIFICATION ACCURACY: A CASE STUDY IN ISTANBUL WITH SENTINEL-2 IMAGES, 508
B. Varol, R. H. Topalolu, E. Sertel

10368- A RESEARCH ON EXTRACTION OF SINGLE 3D BUILDING MODEL FROM OBLIQUE PHOTOGRAPHY DATA ASSISTED BY REMOTE SENSING IMAGES, 514
T. Wan, hun Liu, Yuan Zhou

10854- DISCRIMINATION AND IDENTIFICATION OF IRON DEPOSITS ON REMOTE SENSING DATA USING FEATURE ORIENTED PRINCIPAL COMPONENT SELECTION AND BAND RATIO METHODS: EASTERN TAURUS, TURKEY, 519
M. Trore , T. Çan, S. Tekin

10990- EDGE EFFECTS BETWEEN THE BORDERS OF TWO ADJACENT DIGITAL ELEVATION MODELS, 526
İ. M. Ozulu , T. Gokgoz

11163- ASSESSMENT OF MACHINE LEARNING METHODS FOR SEAGRASS CLASSIFICATION IN THE MEDITERRANEAN, 531
T. Bakirman, M.U. Gumusay



International Symposium on Applied Geoinformatics (ISAG-2019)

EDGE EFFECTS BETWEEN THE BORDERS OF TWO ADJACENT DIGITAL ELEVATION MODELS

Ibrahim Murat Ozulu [1]*, Turkay Gokgoz [2]

[1]Hitit University, Architecture and City Planning Department, Vocational School of Technical Sciences, Çorum, Turkey (imuratozulu@hitit.edu.tr); **ORCID 0000-0002-0963-3600**

[2]Yildiz Technical University, Faculty of Civil Engineering, Department of Geomatics, Istanbul, Turkey (gokgoz/hacar@yildiz.edu.tr); **ORCID 0000-0001-8716-6131**

*Corresponding Author

ABSTRACT: Digital Elevation Models (DEMs) is a collection of elevations (or depths) to represent the terrain surface. DEMs can be derived using elevation data from topographic maps or, directly, from stereo imagery, interferometric synthetic aperture radar or light detection and ranging (LiDAR). However, in case of using elevation data of topographic maps, data volume could be enormous with respect to the processing capacity of Geographical Information Systems (GIS), thus it could not be possible to produce a single DEM. In this case, several map-based DEMs covering the study area could be produced one by one and then merged, but edge effects between the borders of two adjacent DEMs may occur. In order to avoid or decrease the edge effects, DEMs are produced within not the original but the expanded boundaries of maps.

In this study, with the aim of not only detecting the edge effects between the borders of two adjacent DEMs but also testing the approach of producing DEMs within the expanded boundaries of maps to avoid the edge effects, (1) the original 25K map boundaries are expanded to 6000 m, (2) 10-meter resolution DEMs are produced using the elevation and hydrography data within the expanded boundaries, (3) the original 25K map boundaries are expanded to 3000 m, (4) DEMs produced in the second stage are clipped using the boundaries obtained in the third stage, and (5) DEMs obtained in the fourth stage are merged and thus a single (i.e. mosaic) DEM is obtained. Finally, elevations of 1379 cell pairs occurred along the common boundary of DEMs are examined. As a result, the edge effects are decreased significantly by the approach of producing DEMs within the expanded boundaries of maps.

Keywords: *Digital Elevation Models, Edge Effects, Interpolation, Overlapping, Topographic Maps*

1. INTRODUCTION

Digital Elevation Models (DEMs) is a collection of elevations (or depths) to represent the terrain surface. DEMs are one of the most main requirements for a large variety of spatial analysis and modeling problems in environmental sciences.

DEMs can be derived using elevation data from topographic maps or, directly, from stereo imagery, interferometric synthetic aperture radar or light detection and ranging (LiDAR). However, in case of using elevation data of topographic maps, data volume could be enormous with respect to the processing capacity of Geographical Information Systems (GIS), thus it could not be possible to produce a single DEM. In this case, several map-based DEMs covering the study area could be produced one by one and then merged, but edge effects between the borders of two adjacent DEMs may occur. In order to avoid or decrease the edge effects, DEMs are produced within not the original but the expanded boundaries of maps. In the literature, there are several studies on this issue. In these studies, depending on the data volume and DEM resolution, map boundaries are expanded to, for example, 30 – 500 cells (Mills and McLeod, 2013; Joughin et al., URL), 250 – 5000 m (Barnard et al., 2010, Foxgrover and Barnard, 2012, Howat et al., 2014, Rizzoli et al., 2017) and 20 – 60 % (Hasegawa et al., 2000; Buckley et al, 2009; Reeves, 2010; James and Robson, 2014; Bertin et al., 2016; Bohlin et al., 2017; Groom et al., 2018).

In this study, it is aimed not only to detect the edge effects between the borders of two adjacent 10-meter resolution DEMs but also to test the approach of producing DEMs within the expanded boundaries of maps to avoid the edge effects.

2. STUDY AREA AND DATA

Elevation and hydrography data of twelve topographic maps (P22B2, P22B3, P23A1, P23A2, P23A3, P23A4, P23B1, P23B4, O22C3, O23C4, O23D3, O23D4) at scale of 1:25,000 are used (Fig. 1). They are located at middle latitude zone (between 36.250 and 36.625° latitudes) and east-west elongated (between 29.375 and 29.875° longitudes).

All data was obtained from General Directorate of Mapping in Geographic Coordinate System (WGS 1984), i.e. unprojected data (latitude-longitude). DEMs could be produced using unprojected data; however, the results may not be as accurate. The best results will be obtained if all data is stored in the same planar coordinate system. Therefore, all data was transformed to Albers projection using the following parameters.

- False Easting: 0
- False Northing: 0
- Central Meridian: 35.0
- Standard Parallel 1: 36.5
- Standard Parallel 2: 41.0
- Latitude of Origin: 0
- Linear Unit: Meter
- Geographic Coordinate System: WGS 1984
- Datum: WGS 1984
- Prime Meridian: Greenwich
- Angular Unit: Degree

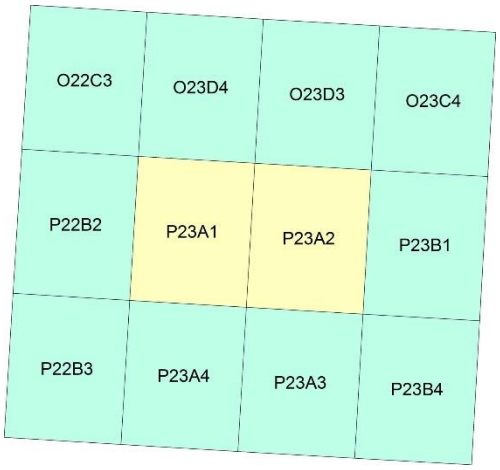

Figure.1 Topographic maps used in this study

3. METHODOLOGY AND EXPERIMENT

In this study, with the aim of not only detecting the edge effects between the borders of two adjacent DEMs but also testing the approach of producing DEMs within the expanded boundaries of maps to avoid the edge effects,

1. The original 25K map boundaries (P23A1 and P23A2) are expanded to 6000 m (Fig. 2),
2. 10-meter resolution DEMs are produced using the elevation and hydrography data within the expanded boundaries (Fig. 3),
3. The original 25K map boundaries are expanded to 3000 m (Fig. 4),
4. DEMs produced in the second stage are clipped using the boundaries obtained in the third stage (Fig. 5), and
5. DEMs obtained in the fourth stage are merged and thus a single (i.e. mosaic) DEM is obtained (Fig. 6).

Finally, elevations of 1379 cell pairs occurred along the common boundary of DEMs were examined. Sample cell pairs are shown in Figure 7.

As a rule of thumb, it is wise to order enough data to provide a 25% overlap surrounding all dimensions of the study area (Reeves, 2010). A 25K map in the study area covers 11×13 km approximately. Accordingly, while east and west boundaries of a map should be expanded to 2750 m, north and south boundaries should be expanded to 3250 m. However, in this study, it is found 3000 m (i.e. the average of 2750 and 3250 m) acceptable for the expansion of all boundaries in all directions. Furthermore, in order to avoid or decrease the edge effects well enough, DEMs are produced within the boundaries obtained by expanding the original map boundaries to 6000 m.

DEMs were produced using ArcGIS Topo to Raster tool. DEMs were merged using ArcGIS Mosaic tool in a way the output cell value of the overlapping areas will be the average value of the overlapping cells.

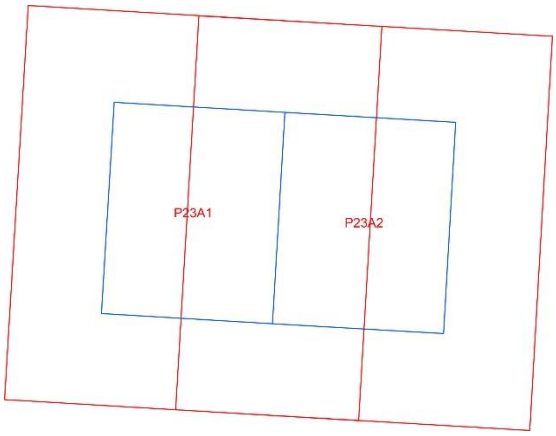

Figure.2 Boundaries obtained by expanding the original 25K map boundaries to 6000 m (red)

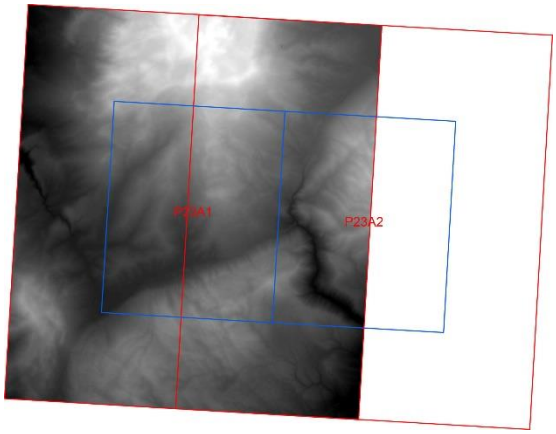

Figure.3 A 10-meter resolution DEM produced using the elevation and hydrography data within the boundaries in Fig. 2

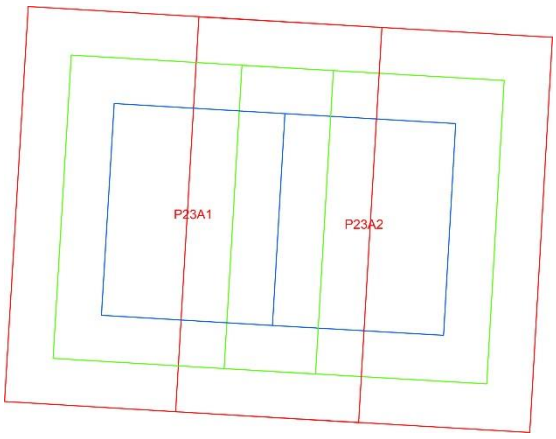

Figure.4 Boundaries obtained by expanding the original 25K map boundaries to 3000 m (green)

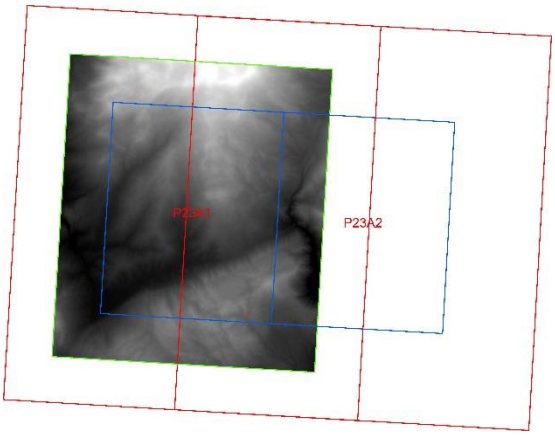

Figure.5 A DEM obtained by clipping DEM in Fig. 3 using the boundaries in Fig. 4.

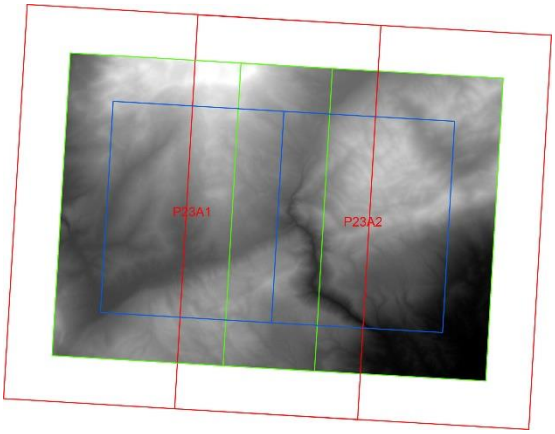

Figure.6 Single (i.e. mosaic) DEM obtained by merging DEMs in Fig. 5

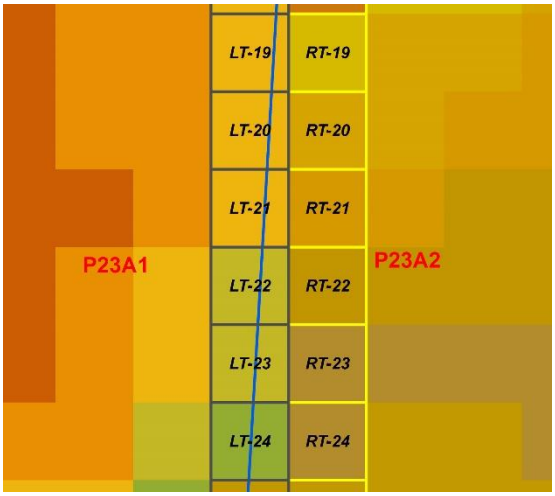

Figure.7 Sample cell pairs

4. RESULTS

Minimum, maximum and average elevation differences between the cell pairs computed from DEM produced within the original map boundaries, hereafter called “Orig Bound DEM”, and DEMs produced within

the expanded boundaries, hereafter called "Expanded Bound DEMs", are given in Table 1. The maximum elevation difference between the cell pairs computed from any Expanded Bound DEM (P23A1, P23A2 or Mosaic) is smaller than that of Orig Bound DEM (Mosaic). As a result, producing DEMs within the expanded map boundaries causes the cell pairs to become closer to each other in elevation. In other words, producing DEMs within the expanded map boundaries causes the surface to become smoother around the common map boundary.

Table 1 Minimum, maximum and average elevation differences between the cell pairs

	Orig Bound	Expanded Bound		
	Mosaic	P23A1	P23A2	Mosaic
Min	0	0	0	0
Max	9.87	6.11	6.11	6.11
Avg	2.69	1.76	1.75	1.75

Minimum, maximum and average of the differences between the elevations of the first cells of all pairs (i.e. the elevations of 1379 cells at left hand side of the common map boundary between P23A1 and P23A2, which were obtained from two different DEMs) are given in Table 2. Similarly, minimum, maximum and average of the differences between the elevations of the second cells of all pairs (i.e. the elevations of 1379 cells at right hand side of the common map boundary between P23A1 and P23A2, which were obtained from two different DEMs) are given in Table 3. Minimum, maximum and average elevation differences were computed as follows. For example, once the difference between two elevations of a cell at left hand side of the common map boundary between P23A1 and P23A2 (e.g. the cell LT-20 in Fig. 7) was computed using its elevations obtained from Orig Bound (P23A1) and Expanded Bound (P23A1), similar process was conduct for the remaining cells at left hand side and thus 1379 elevation differences were obtained. Finally, 0, 6.81 and 0.70 m were determined as the minimum, maximum and average elevation differences, respectively (Table 2).

Table 2 Minimum, maximum and average of the differences between the elevations of the first cells of all pairs (i.e. the elevations of 1379 cells at left hand side of the common map boundary between P23A1 and P23A2, which were obtained from two different DEMs)

			Orig Bound	Expanded Bound	
			P23A1	P23A1	P23A2
Expanded Bound	P23A1	Min	0		
		Max	6.81		
		Avg	0.70		
	P23A2	Min	0	0	
		Max	7.99	2.99	
		Avg	0.71	0.03	
	Mosaic	Min	0	0	0
		Max	7.02	1.49	1.50
		Avg	0.70	0.02	0.02

Average of the differences between the elevations of the first cells of all pairs (i.e. the elevations of 1379 cells at left hand side of the common map boundary between P23A1 and P23A2, which were obtained from Expanded Bound P23A1 and Expanded Bound P23A2) was computed as 0.03 m. It means that two cells appearing in two different DEMs but at the same position are quite close to each other in elevation. As a result, 3000 m is sufficient for producing the overlapping DEMs.

Table 3 Minimum, maximum and average of the differences between the elevations of the second cells of all pairs (i.e. the elevations of 1379 cells at right hand side of the common map boundary between P23A1 and P23A2, which were obtained from two different DEMs)

			Orig Bound	Expanded Bound	
			P23A2	P23A1	P23A2
Expanded Bound	P23A1	Min	0		
		Max	5.60		
		Avg	0.71		
	P23A2	Min	0	0	
		Max	5.54	1.99	
		Avg	0.71	0.03	
	Mosaic	Min	0	0	0
		Max	5.55	0.99	1.00
		Avg	0.71	0.02	0.02

5. CONCLUSION

Since producing DEMs within the expanded map boundaries causes the cell pairs to become closer to each other in elevation, it causes the surface to become smoother around the common map boundary. As a result, in order to avoid the edge effects, DEMs should be produced within the expanded map boundaries. In case of producing 10-meter resolution DEMs using the elevation and hydrography data of topographic maps at scale of 1:25.000, the overlapping area should be 3000 m in extent. Consequently, this study confirms that it is wise to order enough data to provide a 25% overlap surrounding all dimensions of the study area, which is defined as a rule of thumb in the literature.

ACKNOWLEDGEMENTS

The authors would like to thank the Scientific and Technological Research Council of Turkey (TUBITAK) for the financial support given under Project No: 115Y411.

REFERENCES

Barnard, P.L., and Hoover, D. (2010). A seamless, high-resolution coastal digital elevation model (DEM) for southern California. U.S. Geological Survey Data Series 487, 8 p.

Bertin, S., Friedrich, H., and Delmas, P. (2016). A merging solution for close-range DEMs to optimize surface coverage and measurement resolution. Photogramm Eng Rem S, 82(1), 31-40.

Bohlin, J., Bohlin, I., Jonzén, J., and Nilsson, M. (2017). Mapping forest attributes using data from stereophotogrammetry of aerial images and field data

from the national forest inventory. Silva Fennica, 51(2), 1-18.

Buckley, S.J., Schwarz, E., Terlaky, V., Howell, J.A., and Arnott, R.W.C. (2009). Terrestrial laser scanning combined with photogrammetry for digital outcrop modelling. International Archives of the Photogrammetry, Remote Sensing and Spatial Information Science, 38, 75-80.

Foxgrover, A.C., and Barnard, P.L. (2012). A seamless, high-resolution digital elevation model (DEM) of the north-central California coast. U.S. Geological Survey Data Series 684, 11 p.

Groom, J., Bertin, S., and Friedrich, H. (2018). Evaluation of DEM size and grid spacing for fluvial patch-scale roughness parameterisation. Geomorphology, 320, 98-110.

Hasegawa, H., Matsuo, K., Koarai, M., Watanabe, N., Masaharu, H., and Fukushima, Y. (2000). DEM accuracy and the base to height (B/H) ratio of stereo images. International Archives of Photogrammetry and Remote Sensing, 33, 356-359.

Howat, I.M., Negrete, A., and Smith, B.E. (2014). The Greenland Ice Mapping Project (GIMP) land classification and surface elevation data sets. The Cryosphere, 8(4), 1509-1518.

James, M.R., and Robson, S. (2014). Mitigating systematic error in topographic models derived from UAV and ground-based image networks. Earth Surf Proc Land, 39(10), 1413-1420.

Joughin, I., Smith, B., Howat, I., and Scambos, T. Greenland Ice Mapping Project 2 (GIMP-2) Algorithm Theoretical Basis Document: A NASA Measures Project. https://nsidc.org/sites/nsidc.org/files/technical-references/GIMP-ATBD-Version2.pdf.

Mills, S., and McLeod, P. (2013). Global seamline networks for orthomosaic generation via local search. ISPRS J Photogramm Remote Sens, 75, 101-111.

Reeves, R. (2010). Scientific computing tutorial: calculating elevation zone thresholds using ArcMap GIS Version 9.0 and public domain digital elevation models. https://www.nceas.ucsb.edu/files/scicomp/Dloads/GISProgramming/McCainESRI_DEMProcTutorial2010Rev.pdf.

Rizzoli, P., Martone, M., Gonzalez, C., Wecklich, C., Tridon, D.B., Bräutigam, B., Bachmann, M., Schulze, D., Fritz, T., Huber, M., Wessel, B., Krieger, G., Zink, M., and Moreira, A. (2017). Generation and performance assessment of the global TanDEM-X digital elevation model. ISPRS J Photogramm Remote Sens, 132, 119-139.